TIMED Solar EUV Experiment: pre-flight calibration results for the EUV Grating Spectrograph

F.G. Eparvier*, T.N. Woods, G. Ucker, and D.L. Woodraska
Laboratory for Atmospheric and Space Physics, University of Colorado, Boulder, CO 80309-0590

ABSTRACT

The Solar EUV Experiment (SEE) on the Thermosphere Ionosphere Mesosphere Energetics and Dynamics (TIMED) satellite will make measurements of the spectral irradiance of the Sun in the soft x-ray, extreme ultraviolet (EUV), and far ultraviolet (FUV) wavelength range. The EUV Grating Spectrograph (EGS) component of SEE is a 1/4 meter Rowland circle spectrograph with a mechanically-ruled concave grating and a microchannel plate detector with a two-dimensional 1024 x 64 coded anode (CODACON) readout. The EGS covers the wavelength range from approximately 26 to 197 nm. The primary calibration of the instrument was done at the NIST Synchrotron Ultraviolet Radiation Facility (SURF) III on their beam line #2. We will detail the calibration methods and results for the EGS, paying attention to the quantification of sensitivity variations over the instrument's large field of view (12.5˚ x 5.3˚), plus scattered light, second-order, and linearity corrections.

Keywords: ultraviolet instrumentation, satellite instrumentation, solar irradiance instrumentation

1. INTRODUCTION

The goal of the Thermosphere Ionosphere Mesosphere Energetics and Dynamics[1] (TIMED) mission is to characterize the region of the atmosphere between 60 and 180 km above the Earth's surface, an alititude range which encompasses the mesosphere, lower thermosphere, and ionosphere (MLTI). The MLTI is a region where many changes occur in the atmosphere. The major constituents of the atmosphere go from being well-mixed to being diffusively separated. Neutral and ionized minor constituents play major roles in the energy balance and the structure of the MLTI. Energy is deposited into this region of the atmosphere in the form of soft x-ray (0.1–30 nm), EUV (30–120 nm), and FUV (120–200 nm) photons from the Sun, charged particles precipitating downward along magnetic field lines, and gravity waves propogating and breaking from below. These energy sources contribute to the ionization, dissociation, heating, dynamics, and complex ion-neutral chemistry of the MLTI. Variability in these sources can cause significant variability in the MLTI region. For example, the solar irradiance in the soft x-ray and EUV can vary by factors as much as an order of magnitude at certain wavelengths over time scales from as short as minutes to as long as the eleven year solar sunspot cycle. This variability can cause changes in temperature, ionization, and minor species abundance. To understand the MLTI requires quantification and understanding of the variability of the major energy inputs to the region. The purpose of the Solar EUV Experiment (SEE) on the TIMED satellite is to measure the solar radiative energy source into the MLTI.

SEE is designed to make absolute measurements of the solar irradiance and its variability in the wavelength range from approximately 1 nm to 200 nm. To cover this broad spectral range the SEE is comprised of two components, an XUV Photometer System (XPS) which is a series of broad-band photodiodes for the 1 to 31 nm range, and the higher resolution EUV Grating Spectrograph (EGS) which covers from 26 to 197 nm. The overall SEE instrument and the calibration of the XPS component have been previously presented[2,3]. This paper will present the EGS component of SEE and its pre-flight calibration.

2. INSTRUMENTATION

The EGS is designed to measure the absolute solar spectral irradiance in the 26-197 nm wavelength range. It is a normal incidence, quarter-meter, Rowland circle spectrograph with a concave grating with slits at one focus and an array detector at another focus. The housing for the EGS is vacuum tight, and while the instrument is on the ground it is kept evacuated with an attached ion pump to keep the optics and detector free from contaminants and to allow for operation and testing of the open microchannel plate detector. A vacuum door is attached to the front of the instrument at the aperature. The field of view (FOV) of the EGS is 12.5˚ x 5.3˚. There are two design reasons for such a large FOV: the

use of a single-axis gimbal for SEE solar pointing from the spacecraft, and the choice of putting a redundant optical path for calibration within the same component housing. These reasons are discussed in more detail in the following two subsections.

2.1 The SEE pointing and observation plan

The TIMED spacecraft will be inserted into a 625 km alitude circular orbit with a 74.1˚ inclination. The spacecraft is three-axis stabilized in a nadir-pointing orientation. The orbit precesses such that a yaw maneuver is required four times a year to keep the SEE on the sunlit side of the the spacecraft and one of the atmospheric instruments on the dark side. On the SEE instrument the EGS is mounted on a platform which allows fine control pointing in one axis only. The SEE will make observations once per orbit, moving its platform to keep the Sun in the same position in one dimension (α) of the field of view (FOV) of the instruments, but allowing it to drift through the FOV in the other dimension (β). The SEE instruments must therefore have large fields of view in the non-controlled dimension and must be carefully calibrated for variations across that FOV. For the EGS the controlled dimension, α, has a FOV of 5.3˚ while the non-controlled or drift dimension, β, has a FOV of 12.5˚.

Depending on the angle of the plane of the TIMED orbit with the Sun–Earth line (the spacecraft β_{sc} angle, not to be confused with the EGS FOV angle β) the SEE will have solar viewing opportunities varying in length from just over three minutes (when $\beta_{sc}=0$˚) to essentially the entire orbit (when $\beta_{sc}=90$˚). However, the SEE will make solar observations only once per orbit, centered on the middle of the window of opportunity. During a typical orbit of the TIMED spacecraft the SEE Solar Pointing Platform (SSPP) is offset pointed to keep the instrument from looking at the Sun while not making an observation. Just prior to a planned solar observation the platform is rotated so that the Sun is placed in the desired position along the controlled dimension, α, of the FOV. The observation begins when the Sun is located at the desired SSPP position. An observation for the EGS consists of a set of twenty integrations, each ten seconds long. Because it has an array detector, the entire wavelength range of the EGS is sampled simultaneously for each integration. During the 200 seconds of the entire observation the Sun will drift through the non-controlled dimension, β, of the FOV, but the platform will track the Sun, keeping it in the same position in the α dimension of the FOV. How much the Sun drifts in the non-controlled FOV during the observation depends on the orbital β_{sc} angle at the time. When $\beta_{sc}=0$˚ the Sun will drift through the entire 12.5˚ of the FOV during the observation, but when $\beta_{sc}=90$˚ the Sun will stay close to the center of the FOV.

2.2 The redundant channels: two instruments in one

One of the ways to track degradation in an instrument is to have a redundant channel used at a low-duty rate compared to the normal, high-duty channel. Rather than build and fly a completely duplicate instrument, the EGS was designed to have a redundant channel occupying the same space as the normal channel, using the same grating and same detector, but an entirely different slit and entirely different optical path for each channel. Figure 1 illustrates this concept. The EGS has two stationary slits with a moveable aperture to select which slit is opened to view the Sun. Each slit is 25 μm wide and 1 mm high. The SSPP is pointed such that the Sun is offset ±1˚ from the center of the controlled FOV dimension, α, depending on which slit is exposed. This offset pointing guarantees that the sunlight will fall on a different and non-overlapping portion of the grating for each slit. Note that the Sun subtends about half a degree at the distance of the Earth. It also guarantees that the solar spectrum will fall on a different and non-overlapping portion of the two-dimensional array detector. Thus the optical paths of the two channels are separate and degradation of the high-duty channel can be tracked using the low-duty channel. On orbit the plan is to use the normal channel for the regular orbit-by-orbit observations and the redundant channel only on a weekly basis.

The EGS also has a built-in flatfielding lamp (see Figure 1). The lamp is a mercury vapor pen-ray which is mounted outside of the housing of the EGS. A sand-blasted quartz window allows the light from the pen-ray to illuminate the entire detector directly with diffuse light. A narrow band filter between the lamp and the window limits the light to the 185 nm line of mercury. The lamp allows for taking flat fields, thereby tracking location-specific degradation on the two-dimensional array detector. The EGS detector flatfield data indicate highly repeatable pixel-to-pixel variations of about 30%, which is primarily due to imperfect balance of the detector charge amplifier pairs.
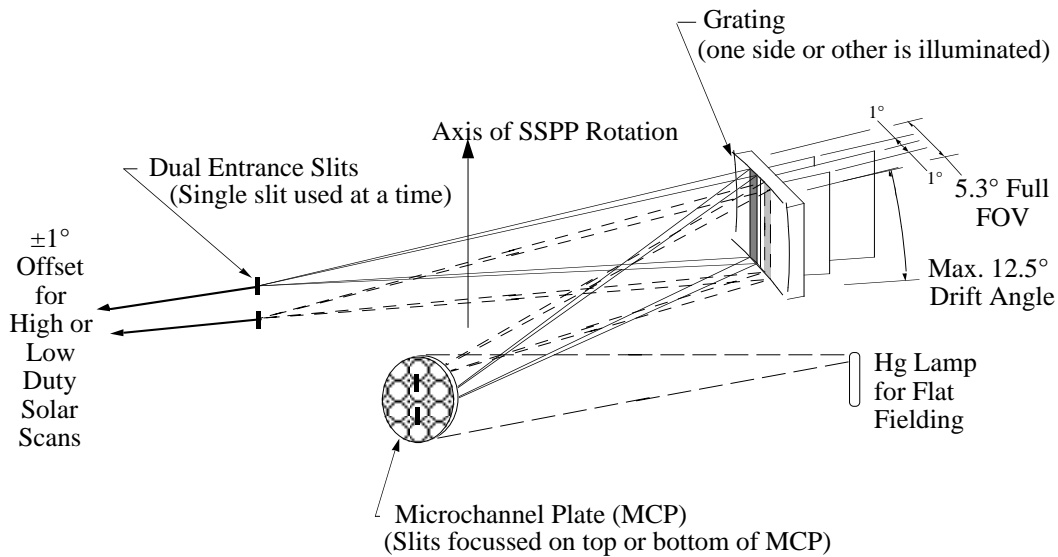
Fig. 1. The optical layout of the EGS showing the two distince optical paths for the high-duty and low-duty channels.

2.3 The detector

The detector for the EGS is a chevron stack of two microchannel plates (MCPs). The MCPs are made by Galileo and have 10 μm diameter micropores with 12 μm center-to-center spacing and a 12˚ bias angle. The MCPs have a gold photocathode. They were chosen after a series of testing[4] showed them to have superior response in the FUV and a greater range of linearity than standard nickel-chromium MCPs with larger micropores. As will be seen in a later section, the detector has a peak in sensitivity in the EUV around 60-80 nm, dropping off fairly rapidly to either side. The resistance of the MCP stack is approximately 26 MΩ at room temperature. The detector readout is a two-dimensional CODACON[5] with 1024 columns (spaced 25 μm center-to-center) and 64 rows (spaced 100 μm). The slit image on the detector is approximately one pixel wide (dispersion direction) and 10 pixels high. The detector is powered by a regulated, stepped high voltage power supply. The voltage across the MCP stack is selectable in seven steps from –1625 V to –1973 V with the nominal setting at –1856 V. The bottom of the MCP stack is held at a voltage of approximately –100 V with respect to the anode (CODACON) plate. In front of the stack are fine wires held at a positive 200 V relative to the top of the MCPs (still negative with respect to ground). In normal applications this mesh is usually held at a negative voltage relative to the top of the MCPs to push escaping electrons down into the micropores, but since the EGS is looking at the bright source of the Sun the few escaping electrons are not a concern and a reverse bias is used to strip them away rather than have them cause potentially mislocated signals on the detector.

2.4 The filters

The EGS has filters which are mounted directly in front of the detector where different wavelengths fall. A MgF_2 window covers about half of the detector, approximately where 117 nm and longward wavelengths of the spectrum fall. Since MgF_2 readily transmits wavelengths of 110 nm and longward, the primary function of this filter is to stop scattered and second order EUV light from falling on the FUV portion of the detector. The end of the MgF_2 window corresponding to about 117 to 127 nm on the dectector is coated with aluminum. The purpose of this metal filter is to cut down the intensity of the hydrogen Lyman-α line at 121.6 nm, which is the brightest emission in the solar spectrum that the EGS detects. The Al filter blocks about 99% of the Lyman-α line so that it will not saturate the detector.

2.5 The grating

The grating in the EGS is made by Hyperfine and is concave, gold coated, and mechanically ruled. The grating has a radius of curvature of 250 mm, and there are 600 grooves/mm across it. The nominal blaze for the grating is for approximately 40 nm. Instead of adjusting the blaze angle for every ruling across the curved surface, the grating is divided into five partitions with the blaze angle varying across each partition. This grating design ultimately causes variations in the sensitivity of the EGS across its field of view. Fortunately, the FOV sensitivity variation due to the partitioning of the grating is most pronounced in the α dimension which is controlled by the movement of the SSPP.

3.   CALIBRATION OVERVIEW

Since the purpose of the SEE is to accurately measure and track solar irradiance variability, knowing the calibration of the instrument during the entire mission is vital. The SEE calibration scheme is threefold: a thorough pre-flight calibration to absolute and repeatable standards, in-flight tracking of relative degradation, and periodic sounding rocket underflights of similar instruments for calibration comparisons. Taking these in reverse order, we will discuss the sounding rocket underflights first.

3.1 Underflight calibrations

During the early phases of the SEE design, prototype EGS and XPS components were built. As part of their development, the prototypes were flown on a sounding rocket from White Sands Missile Range in New Mexico in 1997 to verify solar signal levels. The prototype EGS is nearly identical to the SEE EGS with a grating made from the same master, the same design of detector with the same kind of MCPs and CODACON readout, the same sized slit, and the same optical path. The only significant difference is that the prototype EGS has only a single slit and no slit changer. It is currently planned to fly the prototypes once per year for the duration of the TIMED mission. The value of these flights is that the prototypes can be calibrated thoroughly on the ground both before and after each rocket flight. A comparison can be made between the solar observations of the TIMED SEE and the rocket-borne prototypes. A transfer of calibration from the prototypes to the SEE can be made, and overall degradation in absolute sensitivity can be tracked.

3.2 In –flight calibrations

Multiple methods of on-board tracking of relative degradation of various EGS components are planned. First, and foremost is the redundant channel. Weekly comparisons of solar measurements made with the low-duty channel and the high-duty channel will be made. Since the low-duty channel will have much less exposure (by a factor of about 50), it is not expected to experience exposure-based degradation as rapidly as the high-duty channel. Also on a weekly basis, flatfield images of the entire detector will be made using the on-board mercury lamp. The flatfields will track any location-specific detector degradation. Flatfields can be taken during times when the EGS is not observing the Sun, so no science data will be lost. On a quarterly basis, offset pointing of the SSPP will allow for relative mapping of the FOV in the controlled dimension α, using the Sun as the light source. On an annual basis counting curves of the detector will be made using the flatfield lamp as the source and stepping the detector high voltage power supply through its full range. The mercury lamp has a photodiode monitor, so variations in the lamp output can be removed from the counting curve data. The EGS also has some wavelength overlap with the XPS, namely in the 26 – 31 nm range and at H Ly-α at 121.6 nm. Comparisons between these two SEE components in these overlap ranges will also help track degradation. Finally, the solar spectrum itself, with it's abundance of emission lines will be used to establish the wavelength calibration for each solar observation made and any wavelength shifts can be readily accounted for.

3.3 Pre-flight calibrations

The primary pre-flight sensitivity calibration for the EGS was performed at the National Institute of Standards and Technology (NIST) in Gaithersburg, MD at their Synchrotron Ultraviolet Radiation Facility III (SURF-III). NIST-SURF-III is the standard source for EUV[6]. Synchrotron radiation is a repeatable, calculated standard, so future solar EUV irradiance missions using synchrotron or other radiometric standards for calibration can readily compare measurements with thos of SEE.

The EGS was calibrated at SURF-III's beamline #2, which is a continuous wavelength source of EUV light. The energy of the source can be varied, which changes the shape of the continuum spectrum. The beam current can also be varied, which changes the intensity of the beam. At the end of beamline #2 is a gimbal system upon which the instrument to be calibrated is mounted. The gimbal allows for precise control of the positioning and pointing of the instrument in horizontal, vertical, pitch, and yaw dimensions. The EGS was mounted to this gimbal and connected to the beamline with a welded bellows. The entire SURF beamline is kept under vacuum, as is the interior of the EGS instrument. The vacuum door of the EGS was opened to allow the SURF beam to fall on the entrance aperture. All EGS calibrations were repeated over FOV maps for each of the slit positions. A representative map for one slit is shown in Figure 2. The map for the other slit is a mirror image about the centerline of the map shown. The maps for the two slits share the centerpoint, which was returned to at the beginning and end of each calibration map. All maps were repeated with the

EGS mounted on the SURF milling table in two orthogonal positions to account for the almost 100% polarization of the synchrotron light.
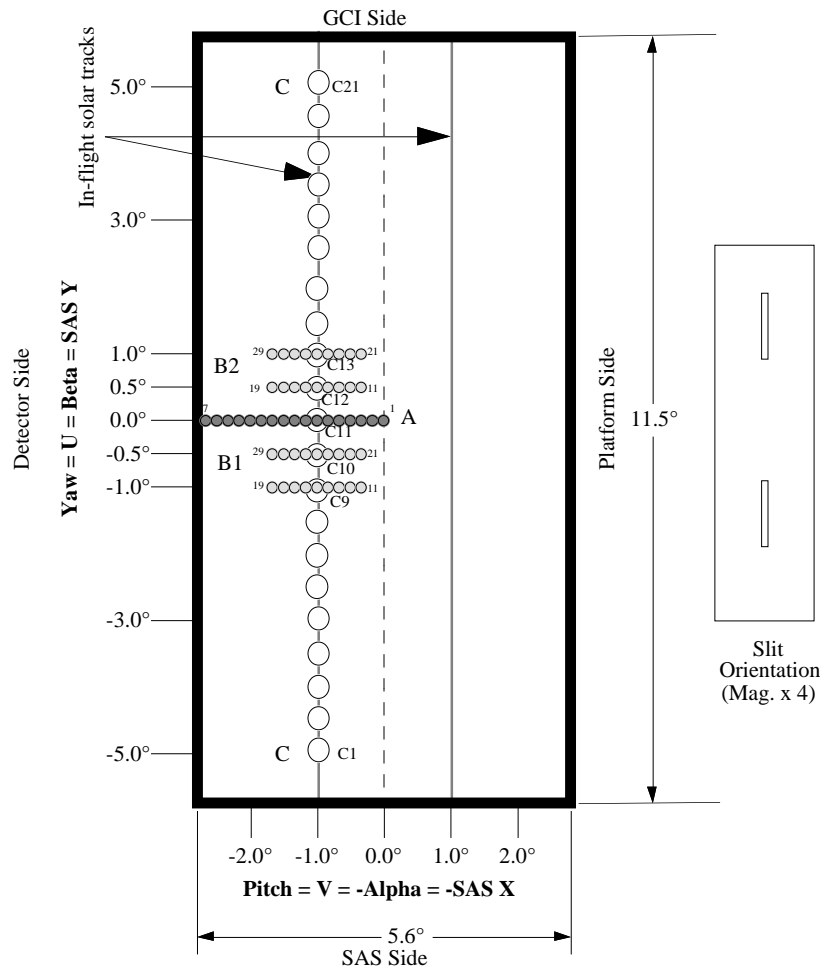

Fig. 2. A representation of the FOV map for the low-duty channel slit.

3.3.1 FUV calibrations

Sensitivity maps were made for the FUV using a beam energy of 362 MeV and beam currents in the 20 to 40 mA range. Integrations of 6 minutes were made at each of the FOV gridpoints marked A on Figure 2, with integrations of 3 minutes at the other gridpoints. CaF_2 filters were placed in the beamline in front of the EGS to eliminate the EUV portion of the SURF spectrum, which is significantly brighter than the FUV portion. The filters were mounted on separate translator stages to allow for easy removal from the beamline. Two filters were used so that filter transmission calibrations could be made before and after each FUV mapping. The quantum throughput for the nominal pointing of one of the slits is shown in Figure 3. Note that the sensitivity of the EGS drops off by roughly two orders of magnitude over the FUV. Fortunately, the solar spectrum rises with wavelength by approximately the same amount over this wavelength range. Figure 4 shows the variations of sensitivity for the EGS over its field of view for a representative FUV wavelength (140 nm). Note that the top panel shows the variations caused by the blaze-angle partitioning of the grating. Recall, though, that this is the dimension in which the SSPP controls the pointing of the instrument, so the nominal pointing for this slit will be at $\alpha=+1°$. The lower panel shows the variation in the sensitivity over the uncontrolled dimension β of the FOV. Note that there are some large variations at the extreme ranges of this dimension, but for most of the orbits the Sun will spent most of its time near the center.
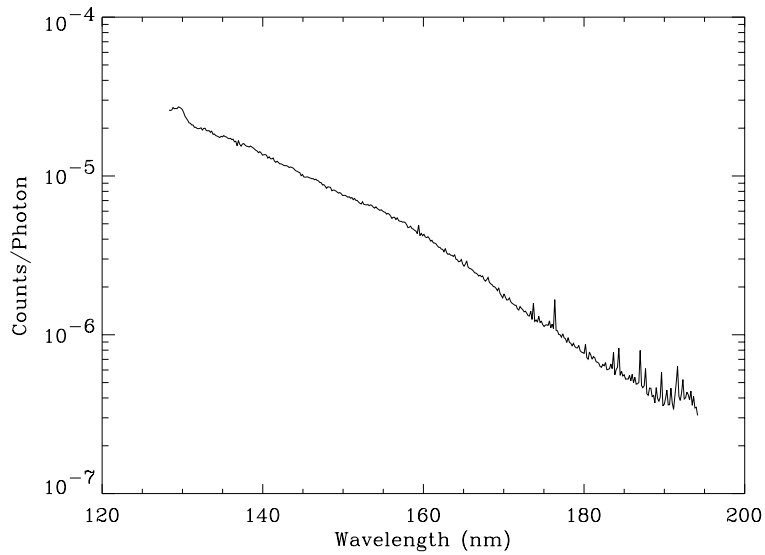
Fig. 3. The quantum throughput (QT) for the FUV portion of the EGS for the nominal pointing of the low-duty channel.
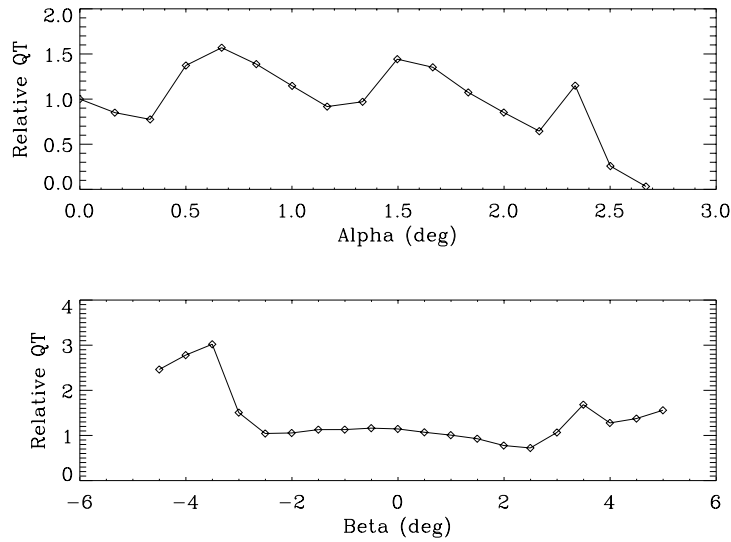

Fig. 4. The FOV variation of the FUV sensitivity of the EGS low-duty channel for a wavelength of 140 nm. The ratio of the sensitivity at each gridpoint to the central point ($\alpha=0°$, $\beta=0°$) is plotted for each. The top panel shows the variation in the controlled dimension α. Note that the nominal pointing for this slit is with $\alpha=+1°$. The bottom panel shows the variation in the drift dimension β.

3.3.2 Second order calibrations

FOV maps were also made using tin filters in front of the EGS for purposes of determining second order effects. The tin filters have a bandpass in the 50 to 80 nm wavelength range, blocking light from other wavelengths. Second order spectra from the tin bandpass are then readily apparent in the EGS data where 100-160 nm would normally fall (note, though that the aluminum and MgF2 filters on the detector block any light longward of 117 nm). A beam energy of 362 MeV and beam currents in the range of 0.20 to 0.35 mA were used for the measurements made with the tin filters, the integration time was 3 minutes for each map point. Figure 5 shows a typical spectrum from the EGS with a tin filter in place showing the second order signal. The ratio of the second order to first order (corrected for wavelength doubling)

for the FOV mapping is shown in Figure 6. Again note the effect of the grating partitions on the variability in the controlled dimension, α. Also again note that the nominal pointing for the slit shown is $\alpha=+1°$.
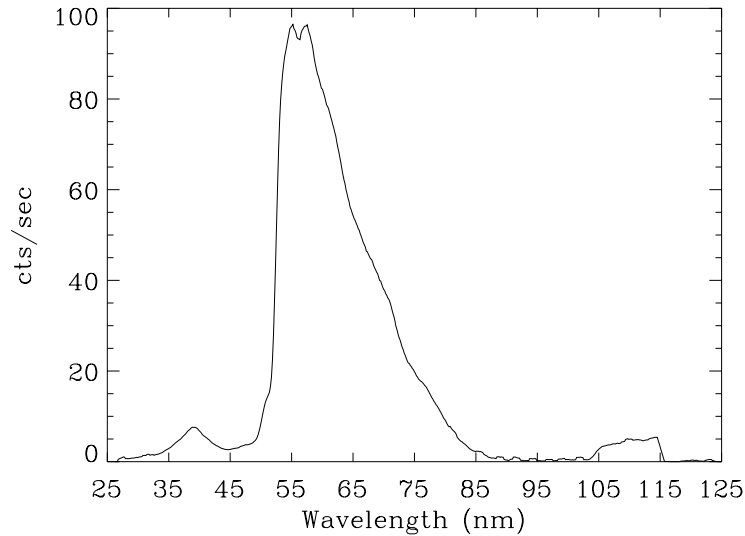
Fig. 5. Sample EGS spectrum of the SURF beam through a tin filter, showing the first order signal from 50-80 nm and the second order signal from 100-117 nm. Note the MgF_2 and Al filters on the detector cut out second order signals longward of 117 nm.
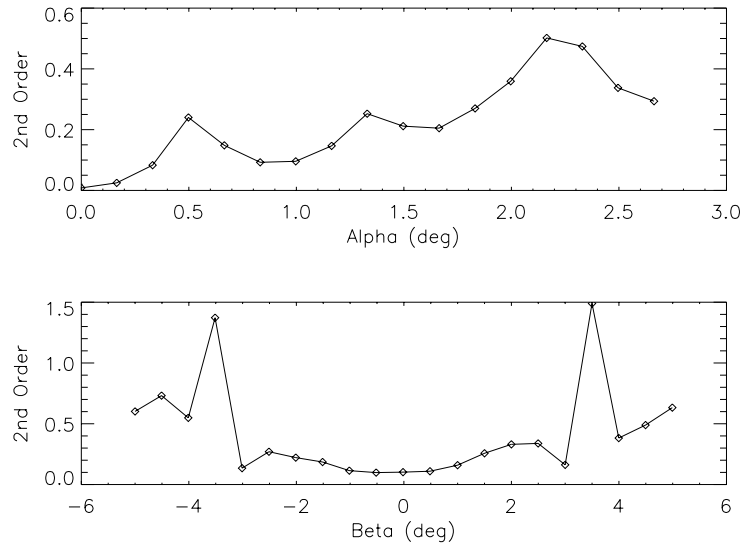

Fig. 6. The FOV map for the second order to first order ratio as determined with the tin filters for the low-duty channel. Shown are the average ratios for the bandpass of the tin filter. The top panel is for the controlled dimension, and the bottom panel is for the drift dimension. Note that the nominal pointing for this slit is with $\alpha=+1°$.

The previously described method of determining second order contributions with tin filters technically only works for the 50-80 nm wavelength range and does not give good wavelength dependence information. Calibration maps using a beam energy of 183 MeV and no filters were also done. Changing the beam energy changes the shape of the SURF spectrum. Comparing the spectra taken with 183 MeV and with 362 MeV beams (with no filters) for each gridpoint allows for a more detailed wavelength dependent determination of the second order contribution. Analyses of this data were still in progress at the time of publication for this paper. They will be reported on in a future paper.

3.3.3 EUV calibrations

Sensitivity FOV map calibrations were made for the EUV portion of the spectrum using a beam energy of 362 MeV and beam currents in the 0.055 to 0.075 mA range. Integration times of 3 minutes were used for all FOV gridpoints. No filters were used for this wavelength range. Analysis of the EUV calibration data requires a correction for second order effects be made. The second order corrections using the tin filter method were applied for this analysis. Figure 7 shows the QT for the EUV portion of the EGS for the same slit as was shown in figure 3. The sensitivity of the EGS is fairly flat across the EUV wavelengths, with a drop off shortward of about 40 nm. Figure 8 shows the FOV variations of the EUV sensitivity for a representative wavelength of 60 nm.
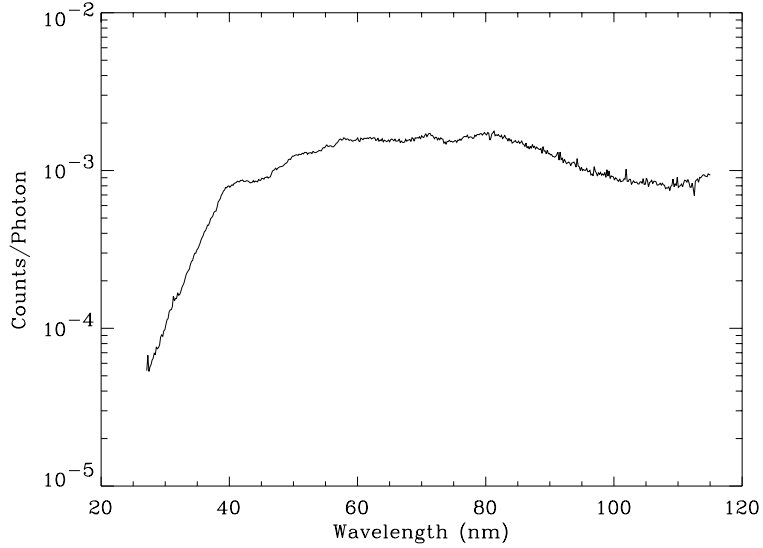
Fig. 7. The quantum throughput (QT) for the EUV portion of the EGS for the nominal pointing of the low-duty channel.
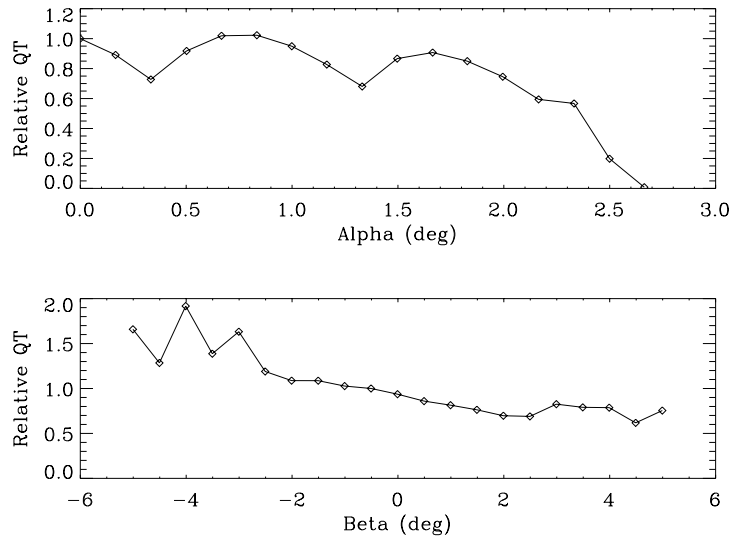
Fig. 8. The FOV variation of the EUV sensitivity of the EGS low-duty channel for a wavelength of 60 nm. The ratio of the sensitivity at each gridpoint to the central point ($\alpha=0°$, $\beta=0°$) is plotted for each. The top panel shows the variation in the controlled dimension α. Note that the nominal pointing for this slit is with $\alpha=+1°$. The bottom panel shows the variation in the drift dimension β.

3.3.4 Scattered light determination

Scattered light corrections are made to all calibration and solar data using the method described by Woods et al.[7] This method redistributes the measured spectrum, correcting for scattered light based on the effective number of grating grooves illuminated and a constant surface roughness scattered light background. The correction is dependent on the FOV angle, the spectral shape, and the solid angle of the incident light. Since the SURF beam has an f/ number of about 1000 while the Sun at the distance of the Earth is approximately f/100, the parameters for correcting the scattered light are different for SURF and solar spectra. These parameters are determined by fitting the spectral data in regions where the signal is dominated by scattered light.

3.3.5 Linearity calibrations

The linearity of the EGS was also measured at SURF-III. This was accomplished by taking data at a wide range of count rates by varying the beam current from 6 mA down to 0 mA. Figure 9 shows the results of this calibration. Note that while the instrument was calibrated for a large range of count rates, the count rates during solar observations are expected to be typically less than 100 counts/second with only a few bright solar lines reaching rates of up to 800 counts/second. As can be seen from the figure, the instrument response is still quite linear for these expected count rates. Also note that the count rates mentioned here are not per pixel on the detector, but are summed up across the height of the slit image on the detector (approximately 10 pixels).
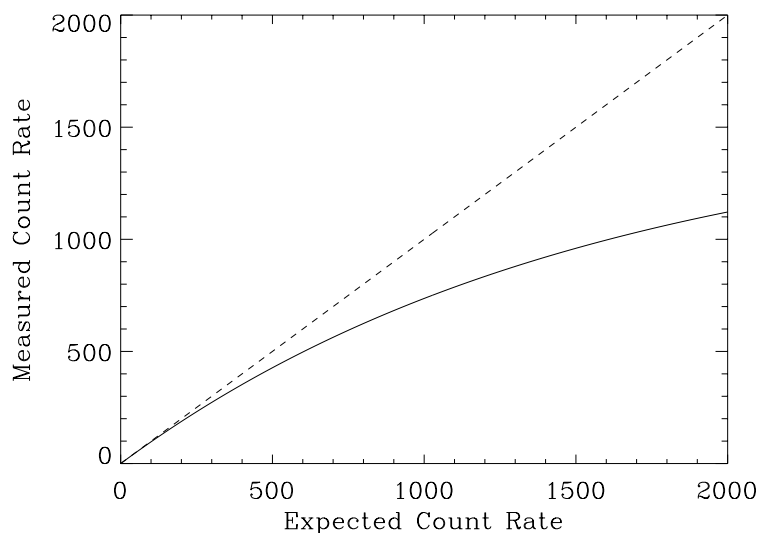
Fig. 9. The linearity of the EGS in counts/second (summed across the 10 pixel height of the slit image on the detector). The dashed line is the response of the instrument in counts/second if it were completely linear at all count rates. The solid curve shows the actual detector response. Note that typical count rates for solar spectra are expected to be less than 100 counts/second with some bright lines possibly reaching 800 counts/second.

3.3.6 Calibration uncertainties

The calculated intensities of the SURF beam incident on the EGS during calibration have an uncertainty of about 0.3% (0.1% from the calculation and 0.2% from the measurement of the beam current at any given time during calibrations). The most significant uncertainties in the sensitivies of the EGS come from sampling statistics (total counts measured at a given wavelength during calibration) and from knowledge of the pointing of the instrument during the FOV maps. The calibration integrations were timed such that the counting statistics gave uncertainties ranging from better than 1% to about 4% depending upon wavelength. The SURF-III beamline #2 gimbal encoders have an uncertainty of about 1 arcminute, which given the variability of our sensitivity over FOV, leads to an additional uncertainty of about 4%.

4. SUMMARY

The EUV Grating Spectrograph is the component of the Solar EUV Experiment on the TIMED satellite which makes measurements of the solar spectral irradiance between 26 and 197 nm. Once launched in the fall of 2001, TIMED will

provide the first daily spectral measurements of the solar EUV since 1981. The broad calibration scheme designed for the SEE, from detailed pre-flight calibrations against synchrotron radiation standards, to on-board degradation checks, and sounding rocket underflights, will assure that the TIMED-SEE measurements will be readily compared to possible future measurements and can be incorporated into a long-term database of solar vacuum ultraviolet irradiance variability measurements.

ACKNOWLEDGEMENTS

* Contact: eparvier@colorado.edu; phone 1-303-492-4546; fax 1-303-492-6444; University of Colorado – LASP, 590 UCB, Boulder, CO USA 80309-0590.

REFERENCES

1. J.-H. Yee, G. E. Cameron, and D. Y. Kusnierkiewicz; "Overview of TIMED," Proceedings of SPIE, Vol. 3756, pp. 244-254 October, 1999.
2. T. N. Woods, F. G. Eparvier, S. M. Bailey, S. L. Solomon, G. J. Rottman, G. M. Lawrence, R. G. Roble, O. R. White, J. Lean, and W. K. Tobiska, "TIMED Solar EUV Experiment", Proceedings of SPIE, Vol. 3442, pp.180–191, October, 1998.
3. T. N. Woods, E. M. Rodgers, S. M. Bailey, F. G. Eparvier, and G. J. Ucker, "TIMED Solar EUV Experiment: preflight calibration results for the XUV photometer system," Proceedings of SPIE, Vol. 3756, pp. 255-264, October, 1999.
4. V. A. Drake, F. G. Eparvier, W. E. McClintock, T. N. Woods, G. J. Ucker, and C. Hill, "Microchannel plate performance and life-test results for the TIMED Solar EUV experiment," Proceedings of SPIE, Vol. 3445, pp. 603-614, November, 1998.
5. G.M. Lawrence and W. E. McClintock, "Compact Ultraviolet Imaging Microchannel Plate Detectors using CODed Anode CONverter (CODACON) Readout Systems", Proceedings of SPIE, Vol. 2831, pp. 104-111, November, 1996.
6. A. C. Parr and S. Ebner, "SURF II User Handbook", NBS Special Publication, Gaithersburg, MD, 1987.
7. T. N. Woods, R. T. Wrigley, and R. E. Haring, "Scattered light properties of diffraction gratings," Applied Optics, vol. 33, pp.4273, 1994.